ELSEVIER

Nuclear Instruments and Methods in Physics Research B 195 (2002) 329–338

NIM B
Beam Interactions with Materials & Atoms

www.elsevier.com/locate/nimb

Molecular dynamics simulation of thin film nucleation through molecular cluster beam deposition: Effect of incident angle

Yanhong Hu, Susan B. Sinnott *

Department of Materials Science and Engineering, University of Florida, 154 Rhines Hall, P.O. Box 116400, 32611-6400 Gainesville, FL, USA

Received 16 October 2001; received in revised form 27 March 2002

Abstract

Deposition of organic cluster beams on solid substrates leads to the creation of thin films through rapid chemical reactions, which makes the process suitable for study by molecular dynamics (MD) simulations. In this work, angular effects of molecular organic beam deposition are studied extensively through classical MD simulations. The reactive empirical bond potential parameterized by Brenner is used. The specific system that is examined consists of an ethylene molecular cluster beam that is deposited on a hydrogen-terminated diamond (1 1 1) substrate at room temperature. The beam impacts the substrate along two crystallographic orientations at incident angles of 0°, 15°, 45° and 60° from the surface normal. Two sets of conditions are considered: one where the total incident energy is constant and one where the momentum normal to the surface is constant. The results are seen to depend on the total energy and incident angle and to be independent of crystallographic orientation.

PACS: 71.15.D; 68.55; 81.15
Keywords: Organic cluster beam deposition; Angle effects; Thin film nucleation; Molecular dynamics simulations

1. Introduction

Cluster deposition on solid substrates to produce high quality thin films has received growing attention over the last two decades [1–16]. In cluster beam deposition, clusters composed of a few atoms to thousands of atoms are ionized and accelerated by applied electric fields to form energetic beams that are then directed to a substrate. Upon deposition, large numbers of atoms are forced briefly together and a high amount of energy is concentrated on a relatively small area of the surface. Often, the incident energy is in the "hyperthermal" energy region such that the energy of the constituent particles of the cluster is about 10–100 eV. In this energy region the interaction between the cluster and the substrate occurs just near the surface and the clusters do not penetrate deeply into the bulk. As a result, there is relatively little

* Corresponding author. Tel.: +1-352-846-3778; fax: +1-352-846-3355.
E-mail address: ssinn@mse.ufl.edu (S.B. Sinnott).

0168-583X/02/$ - see front matter © 2002 Published by Elsevier Science B.V.
PII: S0168-583X(02)01135-7

damage to the substrate. This method is therefore well suited to generate thin films [2–5] and also has found promising applications in surface modification such as surface smoothing [2,6].

It is possible to generate different products when the operating parameters such as the incident energy, impact species, incident angle, substrate structure and the ambient conditions are changed. Among all those factors, the effect of incident angle has received some attention. For example, the influence of the angle on the kinetic energy distribution of molecular fragments sputtered from polymer substrates under indium ion bombardment [7] has been examined. It was found that the energy spectra of the fragment ions obtained at 2 keV with an impact angle of 65° were broader than those observed at higher energy and lower impact angle [7]. By using target current measurements to determine ion-induced electron yields of silicon bombarded with N_2^+ ions at angles between 0° and 84°, it was found that with increasing angle, the yields of nitrogen-saturated samples first increased and then decreased rather rapidly at some critical angle [8]. Furthermore, ripples grew rapidly at angles between 37° and 75°, which strongly increased the electron yields [8]. The incident angle dependence of the sputtering effect of Ar cluster beam deposition has also been considered [1]. The experimental results showed that the sputtering yield decreased as the incident angle increased in a manner proportional to $\cos\theta$. In addition, the roughness of the Cu surface monotonically increased as the incident angle increased [1].

Computer simulations have played an active role in understanding the dynamic processes that occur in cluster–surface deposition at the atomic scale, guiding experiments to obtain desirable surface morphologies, and predicting the crystalline microstructures of deposited films. Besides the above-mentioned experimental work, computer simulations also reveal the influence of the incident angle on the process. For instance, molecular dynamics (MD) simulations have been used to study the effect of incident angle on the deposition of Al clusters, and the results indicated that depending on the angle and energy, atoms in the substrate exhibited highly directional or more diffused thermal vibrations [9]. Kinetic Monte Carlo simulations have also been used to study the effect of varying deposition angles of a molecular beam on the morphology of a growing film [10]. It was demonstrated that the density of the film decreased with increasing incident angle because of the formation of pores and the growth of columnar structures [10].

In this paper the angular dependence of organic molecular cluster beam deposition at hyperthermal energies is considered using MD simulations. The effects of incident energy and impact orientation on the angular dependence of the nucleated thin films are also investigated. This builds on previous work where MD simulations were used to show how cluster molecular species [11,12], incident kinetic energy [11–13], cluster size [14], beam type [15], surface reactivity [16] and substrate temperature [15] influence the nucleation and growth of hydrocarbon thin films.

2. Computational details

To model the interatomic interaction between carbon atoms and between carbon and hydrogen atoms, the modified reactive empirical bond order (REBO) potential for hydrocarbons parameterized by Brenner is used [17,18]. The potential energy is written as a sum of effective pair terms for each bond, and includes a many-body term that takes into account the chemical environment of each bond. It allows for bond breaking and new bond formation in a realistic manner [19,20] and thus is well suited to study hydrocarbon deposition on diamond or graphite substrates. However, as is true with most empirical potentials, there are cases where the predictions provided by the REBO potential do not agree perfectly with ab initio or quantum-based tight-binding predictions, although the qualitative trends are correct [21–23]. Nevertheless, it allows for the treatment of thousands of atoms in a relatively short amount of time on standard workstations rather than using large amounts of time on massively parallel computers. In the case of the present study, the system sizes are too large to allow for the use of more accurate ab initio or tight-binding approaches, even with the use of supercomputers.

Since the REBO potential is only effective in the short (covalent bond) range, Lennard-Jones (LJ) potentials are coupled to the REBO potential to describe the long range van der Waals interactions present in the molecular clusters. Thus, the combined expression for the binding energy (E_b) between atoms i and j can be expressed in the form

$$E_b = \sum_i \sum_{j(>i)} [V_R(r_{ij}) - B_{ij} V_A(r_{ij}) + V_{vdw}(r_{ij})], \quad (1)$$

where V_R and V_A are pair-additive interactions that model the interatomic repulsive and attractive forces, respectively; V_{vdw} is the contribution from long-range van der Waals interactions; r_{ij} is the distance between atoms i and j; and B_{ij} is a many-body empirical bond-order term. V_{vdw} is only non-zero after the REBO potential has gone to zero. More details about this potential and the coupling between the REBO and LJ potentials are provided elsewhere [17,18,23].

The ethylene molecular cluster beam used in each trajectory consists of 20 clusters, where each cluster contains eight ethylene molecules. An initial ethylene cluster, which is used as the starting cluster to build the beam, is fully relaxed and quenched to 5 K to minimize the internal cluster kinetic energy. The beam is then built through the repetition of that initial cluster in different translational and angular orientations relative to each other and the surface. The distance between the adjacent clusters is about 4 Å. In each trajectory the whole beam is initially placed about 4 Å above the underlying substrate where the interactions between the cluster and the substrate atoms are negligible.

The substrate considered here is a hydrogen-terminated diamond (1 1 1) surface that is made up of 24 layers of carbon atoms terminated at the top and bottom with hydrogen. This substrate has been shown to prevent the unphysical rebounding of energy from interfering with the chemical reactions at the surface at high deposition energies [24]. The substrate contains 13 700–13 900 atoms with an impact plane area of 69 × 40 Å^2. Two-dimensional periodic boundary conditions are applied within the plane of the surface to mimic a semi-infinite system. Prior to the beam deposition, the substrate is fully equilibrated at 500 K and then cooled to the deposition temperature of 300 K. In order to achieve the ideal simulation environment, the surface atoms are divided into three different types. The bottom layer of hydrogen atoms is held rigid to maintain the structure. The next six carbon layers and 5–6 rows of atoms at the edges of the slab are set to be thermostat atoms, which have Langevin frictional forces applied to them. These thermostat atoms dissipate the extra energy that is pumped into the surface during deposition and thus maintain the system temperature at close to 300 K. The other surface atoms and all the cluster beam atoms respond to the applied forces without any further constraints. Fig. 1 shows the arrangement of the thermostat atoms and the normal atoms in the substrate.

The cluster beam is deposited onto the substrate along two different crystallographic orientations of the surface, $[\bar{1}\,\bar{1}\,2]$ and $[\bar{1}\,1\,0]$, hereafter referred to as (I) and (II), respectively, at incident angles, θ, of 0°, 15°, 45° and 60° with respect to the surface normal, as shown in Fig. 2. Two incident energies, 25 eV/cluster-molecule and 50 eV/cluster-molecule, are considered. When θ varies from the surface normal, the energy deposited along the surface normal also changes according to the following relationship of the total incident energy (E_{total}), the amount of energy that is pumped into the surface, which is equivalent to the normal momentum (E_{normal}), and the incident angle,

$$E_{normal} = E_{total} \cos^2 \theta. \quad (2)$$

Therefore cases where the amount of energy that is pumped into the surface is kept at a constant value of 50 eV/cluster-molecule are also studied. Thus, five unique cases are considered in this work: total impact energy of 50 eV/cluster-molecule along the (I) crystallographic orientation; constant normal impact energy of 50 eV/cluster-molecule along the (I) crystallographic orientation; total impact energy of 50 eV/cluster-molecule along the (II) crystallographic orientation; constant normal impact energy of 50 eV/cluster-molecule along the (II) crystallographic orientation and total impact energy of 25 eV/cluster-molecule along the (I) crystallographic orientation. All the simulations run for 3 ps and the time-step used is 0.2 fs. For

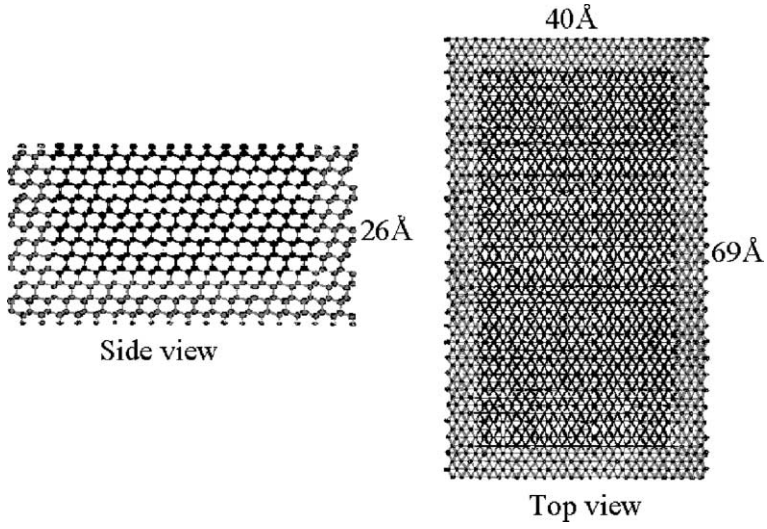

Fig. 1. The arrangement of thermostat atoms (grey) and normal atoms (black) within the substrate.

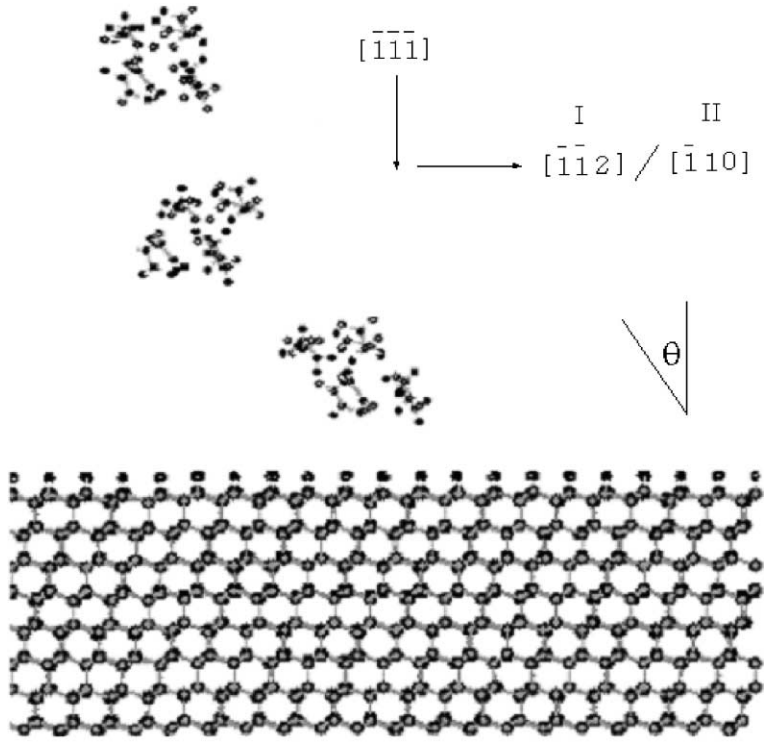

Fig. 2. A representative snapshot of the system prior to deposition of the cluster beam (only part of the cluster beam and the substrate are shown for clarity).

statistical purposes, five separate trajectories that use different impact points are considered for each of the five cases listed above. The averaged results and the standard deviations are reported.

3. Results

Numerous chemical reactions occur among the cluster molecules and between the cluster and the substrate, resulting in amorphous hydrocarbon thin film nucleation and growth. The simulations also indicate that many cluster molecules and products of the chemical reactions scatter away from the surface and that, as the film nucleates and begins to grow, portions of it are sputtered away. The percentage of incident cluster carbon atoms that adhere to the surface after deposition at various incident angles for the five cases considered is shown in Table 1 and Fig. 3. When the total impact energy is the same (25 eV/cluster-molecule or 50 eV/cluster-molecule) along the (I) crystallographic orientation, the amount of adhesion of the cluster molecules, or the products of their chemical reactions, decreases monotonically as the incident angle increases, although the results of the deposition at 15° in each case is about the same as the corresponding normal impacts. This decrease is due to the decrease in the amount of energy pumped into the surface as the angle increases from the surface normal.

Table 1
The percentage of carbon atoms in the incident beam that adhere to the surface (%)

	Case A	Case B	Case C	Case D	Case E
0°	53.75 ± 4.49		52.00 ± 3.74		18.44 ± 4.18
15°	49.81 ± 3.98	55.38 ± 2.28	53.56 ± 3.83	54.31 ± 5.39	16.25 ± 3.83
45°	25.38 ± 4.90	47.13 ± 5.47	32.00 ± 6.21	48.25 ± 3.98	6.00 ± 1.99
60°	11.06 ± 1.22	32.38 ± 3.19	11.69 ± 2.28	30.31 ± 3.78	1.88 ± 2.80

Case A corresponds to impact along the (I) crystallographic orientation at constant total impact energy of 50 eV/cluster-molecule. Case B corresponds to impact along the (I) crystallographic orientation at constant normal impact energy of 50 eV/cluster-molecule. Case C corresponds to impact along the (II) crystallographic orientation at constant total impact energy of 50 eV/cluster-molecule. Case D corresponds to impact along the (II) crystallographic orientation at constant normal impact energy of 50 eV/cluster-molecule. Case E corresponds to impact along the (I) crystallographic orientation at constant total impact energy of 25 eV/cluster-molecule.

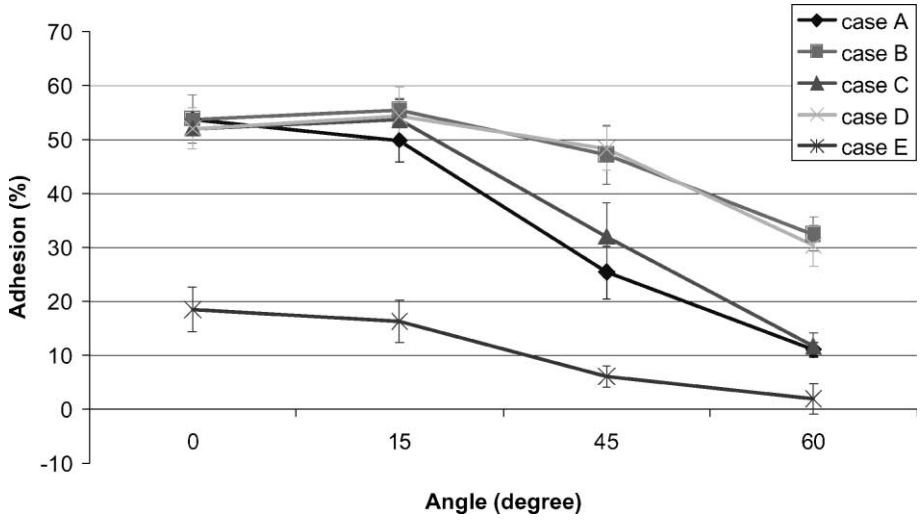

Fig. 3. Percentage of carbon atoms in the ethylene cluster beam that adhere to the substrate on deposition as a function of incident angle. (Case A: impact along the (I) crystallographic orientation at constant total impact energy of 50 eV/cluster-molecule; Case B: impact along the (I) crystallographic orientation at constant normal impact energy of 50 eV/cluster-molecule; Case C: impact along the (II) crystallographic orientation at constant total impact energy of 50 eV/cluster-molecule; Case D: impact along the (II) crystallographic orientation at constant normal impact energy of 50 eV/cluster-molecule; Case E: impact along the (I) crystallographic orientation at constant total impact energy of 25 eV/cluster-molecule).

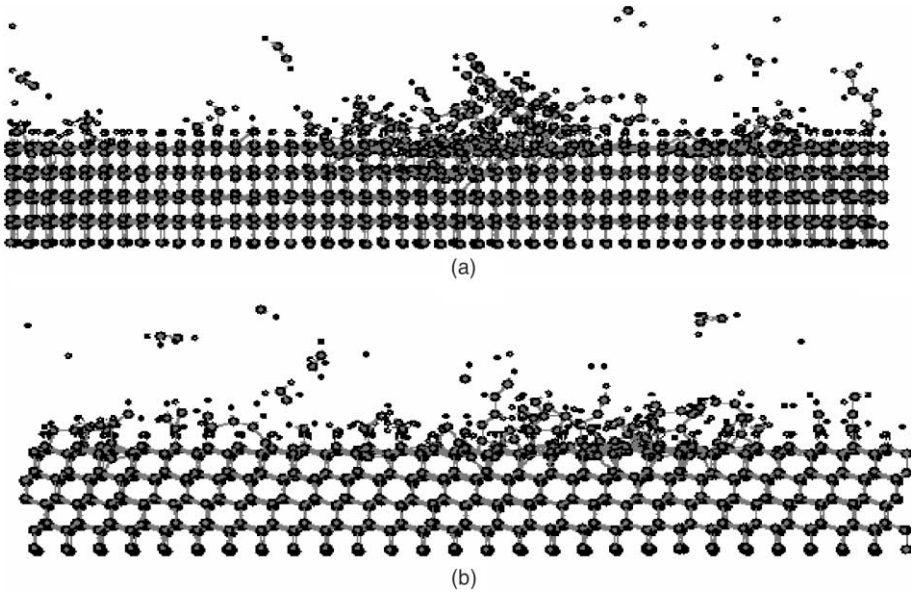

Fig. 4. Snapshots from the MD simulations of the nucleated thin films as a result of ethylene cluster beam deposition: (a) from a simulation where the total incident energy is 50 eV/cluster-molecule along the (I) crystallographic orientation at 15° and (b) from a simulation where the total incident energy is 50 eV/cluster-molecule along the (II) crystallographic orientation at 45°.

For this reason, cluster beam deposition at constant normal energies of 50 eV/cluster-molecule are also studied. In this case, according to Eq. (2), the total impact energy increases as the angle increases such that it becomes quite high at large incident angles (for example, the total energy doubles at 45° compared to at 0°). Under these conditions, the adhesion percentage is about the same for the 0°, 15° and 45° deposition cases, as shown in Fig. 3 and Table 1. However, in the 60° deposition case, the adhesion percentage decreases, although the decrease is not as dramatic as before.

Deposition along the (II) crystallographic orientation yields the same trends, as indicated in Fig. 3 and Table 1. The adhesion percentages along different crystallographic orientations at the same angles are approximately the same within the standard deviation of the results. This indicates that the chemical reactions and adhesion that leads to thin-film nucleation and growth have little dependence on the crystallographic orientation of the incident beam.

Typical snapshots of the nucleated thin films along the (I) and (II) crystallographic orientation depositions are shown in Fig. 4(a) and (b), respectively. The thin films grow mainly in the direction of beam deposition. The structure of the nucleated film is analyzed quantitatively by determining the atomic coordination (Table 2) and carbon connectivity (Table 3) of the carbon atoms in the film. Carbon connectivity is the manner in which the carbon atoms in the film connect to other carbon atoms in the film. Linear structures are indicated when carbon atoms are connected to one or two other carbon atoms, branched structures are indicated when the carbon atoms are connected to three carbon atoms, while networked structure are indicated when the carbon atoms are connected to four carbon atoms.

A close examination of Tables 2 and 3 reveals that the incident angle has little effect on either the coordination or carbon connectivity when deposition occurs at constant total incident energy. In the case of deposition at constant normal energy, as the angle changes, few variations in the carbon connectivity are seen (Table 3). However, with increasing angle, the percentage of sp^3-hybridized atoms decreases while the percentage of sp-hybridized atoms increases (Table 2). Deposition

Table 2
The coordination percentage of the film carbon atoms (%)

	0°	15°	45°	60°
Case A				
1 neighbor	0.90 ± 0.50	1.90 ± 1.06	2.49 ± 1.76	6.81 ± 2.98
sp	22.30 ± 1.30	21.62 ± 2.80	25.12 ± 8.36	36.65 ± 9.55
sp^2	46.06 ± 5.88	50.71 ± 3.32	47.51 ± 10.00	39.27 ± 16.86
sp^3	30.74 ± 6.80	25.77 ± 6.18	24.88 ± 6.58	17.28 ± 8.60
Case B				
1 neighbor	0.90 ± 0.50	1.40 ± 0.82	6.51 ± 2.21	13.18 ± 2.52
sp	22.30 ± 1.30	23.60 ± 2.10	35.43 ± 6.93	45.29 ± 3.01
sp^2	46.06 ± 5.88	51.62 ± 5.46	47.17 ± 10.05	35.98 ± 17.47
sp^3	30.74 ± 6.80	23.38 ± 5.04	10.89 ± 5.55	5.55 ± 1.13
Case C				
1 neighbor	2.02 ± 0.85	1.16 ± 1.08	2.91 ± 3.06	4.35 ± 2.02
sp	23.21 ± 1.02	19.33 ± 2.70	28.68 ± 7.30	35.27 ± 6.53
sp^2	51.91 ± 7.50	53.01 ± 8.21	42.05 ± 18.32	40.58 ± 13.05
sp^3	22.87 ± 3.02	26.50 ± 8.45	26.36 ± 6.26	19.81 ± 8.61
Case D				
1 neighbor	2.02 ± 0.85	1.66 ± 0.78	6.97 ± 2.19	13.15 ± 3.28
sp	23.21 ± 1.02	23.84 ± 4.67	39.07 ± 6.34	40.06 ± 3.85
sp^2	51.91 ± 7.50	50.11 ± 3.63	43.29 ± 7.94	40.46 ± 7.72
sp^3	22.87 ± 3.02	24.39 ± 6.43	10.67 ± 2.70	6.33 ± 1.26
Case E				
1 neighbor	0.69 ± 0.94	0.39 ± 0.87	–	Too few film atoms
sp	11.38 ± 7.38	8.53 ± 2.60	10.42 ± 3.68	to consider
sp^2	34.14 ± 8.21	32.95 ± 10.88	39.58 ± 31.38	
sp^3	53.79 ± 12.69	58.13 ± 14.04	50.00 ± 17.12	

Case A corresponds to impact along the (I) crystallographic orientation at constant total impact energy of 50 eV/cluster-molecule. Case B corresponds to impact along the (I) crystallographic orientation at constant normal impact energy of 50 eV/cluster-molecule. Case C corresponds to impact along the (II) crystallographic orientation at constant total impact energy of 50 eV/cluster-molecule. Case D corresponds to impact along the (II) crystallographic orientation at constant normal impact energy of 50 eV/cluster-molecule. Case E corresponds to impact along the (I) crystallographic orientation at constant total impact energy of 25 eV/cluster-molecule.

along different crystallographic orientations does not yield any significant differences.

Because of the large mass and high energy density deposited locally during energetic cluster deposition, the substrate experiences some damage. Despite the rigid nature of the diamond used in this study, the substrate deforms on impact at all the incident energies used here. In all cases, the damage or deformation of the surface occurs through the displacement, or kicking-out, of surface atoms centered on the point of cluster beam deposition. No obvious craters are formed in any of the cases considered. The main mechanism of such damage production, as suggested by Ghaly et al. [25], is ballistic damage, which is created by the direct knock of atoms onto the surface as in the binary collision mechanism. The overall deformation of the surface decreases as the angle increases when the cluster beam impacts at the constant total incident energy. At lower energies (of 25 eV/cluster-molecule versus 50 eV/cluster-molecule) less deformation occurs at normal or near-normal deposition. In the cases where the normal incident energy is kept constant as the angle increases, the damage to the substrate becomes more severe as the angle increases, especially in the lateral direction.

4. Discussion

Our previous studies have shown that the adhesion of incident species increases with increasing

Table 3
The percentage of carbon connectivity of the film carbon atoms

	0°	15°	45°	60°
Case A				
Linear	82.43 ± 9.46	81.71 ± 5.81	91.55 ± 19.73	87.96 ± 12.08
Branched	16.78 ± 2.05	17.58 ± 3.65	9.45 ± 3.47	12.04 ± 6.03
Networked	0.79 ± 1.23	0.71 ± 0.50	–	–
Case B				
Linear	82.43 ± 9.46	79.52 ± 3.55	79.51 ± 6.78	77.40 ± 5.05
Branched	16.78 ± 2.05	19.94 ± 4.16	19.96 ± 3.97	21.41 ± 4.63
Networked	0.79 ± 1.23	0.54 ± 0.38	0.53 ± 0.53	1.19 ± 1.43
Case C				
Linear	79.51 ± 4.32	81.11 ± 6.67	89.92 ± 17.58	83.57 ± 16.52
Branched	19.23 ± 3.37	18.19 ± 4.59	9.11 ± 3.33	16.43 ± 9.72
Networked	1.26 ± 1.18	0.70 ± 1.21	0.97 ± 0.69	–
Case D				
Linear	79.51 ± 4.32	82.12 ± 10.55	76.98 ± 9.48	71.88 ± 4.30
Branched	19.23 ± 3.37	17.22 ± 3.01	22.18 ± 4.42	26.41 ± 5.31
Networked	1.26 ± 1.18	0.66 ± 0.46	0.84 ± 0.47	1.71 ± 0.84
Case E				
Linear	97.25 ± 23.39	96.12 ± 24.07	97.92 ± 32.43	Too few film atoms
Branched	2.75 ± 1.96	3.88 ± 2.74	2.08 ± 4.66	to consider
Networked	–	–	–	

Case A corresponds to impact along the (I) crystallographic orientation at constant total impact energy of 50 eV/cluster-molecule. Case B corresponds to impact along the (I) crystallographic orientation at constant normal impact energy of 50 eV/cluster-molecule. Case C corresponds to impact along the (II) crystallographic orientation at constant total impact energy of 50 eV/cluster-molecule. Case D corresponds to impact along the (II) crystallographic orientation at constant normal impact energy of 50 eV/cluster-molecule. Case E corresponds to impact along the (I) crystallographic orientation at constant total impact energy of 25 eV/cluster-molecule.

deposition energy [11–13] at normal impacts. Therefore, in these previous studies all the incident energy is transferred directly to the substrate atoms. This work again shows that higher normal momenta lead to greater adhesion and hence film nucleation and growth. In addition, when the beam is deposited at various angles with constant normal energy, adhesion remains almost constant up to 45°. But for larger angles, the amount of adhesion decreases. Therefore, although previous work and this study both suggest that the normal momentum is important to determine the amount of thin-film adhesion, this work shows that the incident angle is another important factor, especially at large angles.

However, the incident angle is predicted to have little influence on the nucleated thin film structure according to the simulation results. One might argue that when the deposition occurs with constant normal energy, the percentage of sp^3-hybridized atoms decreases while the percentage of sp-hybridized atoms increases (Table 2) with increasing incident angle. However, this could be due to the changes in the total energy rather than to the incident angle. This is because when the normal deposition energy is the same for different incident angles, the total energy increases with increasing angle, as shown in Eq. (2). Previous work has shown that when the deposition energy increases, ethylene cluster beam deposition tends to generate hydrocarbon thin films with less sp^3-hybridization but more sp-hybridization [11–13]. The set of simulations presented here indicate that the total incident energy rather than the normal momentum affects the coordination of the carbon atoms in the nucleated thin film.

Crystallographic orientation is another factor studied in this work. It is found that deposition

along different orientations does not affect either the adhesion percentage or the structure of the nucleated thin film. This is because when the beam is generated, the molecules in each cluster and the positions of the clusters in the whole beam are randomized. Therefore, upon deposition, different molecules and clusters impact the substrate in different directions as well as different places. So the overall effect appears to be isotropic.

Studying the damage to the substrate upon deposition reveals the correlation of the incident energy and angle. In angled deposition, the damage to the substrate surface can be divided into two components, perpendicular damage and horizontal damage, which are attributed to the normal and horizontal momenta of the cluster, respectively. When the total incident energy is held fixed, as the incident angle increases, the normal momentum decreases and the horizontal momentum increases. Therefore, the ''depth'' of the surface damage or deformation of the surface decreases as the angle increases, although there might be more lateral deformation. However, when the angular deposition occurs with the same normal incident energy, the overall deformation of the surface becomes more severe because of the higher momentum transferred to the surface atoms with increasing incident angle. Therefore, under these conditions, the damage to the substrate becomes more severe with increasing angle.

5. Conclusions

This study examines the angular effects of ethylene molecular cluster beam deposition at various incident energies along two crystallographic orientations of hydrogen-terminated diamond (1 1 1) surface using classical MD simulations with a reactive empirical potential coupled to a LJ potential. It predicts that deposition at small angles ($\leqslant 15°$) will generate nucleated organic thin films similar to those that are formed at normal deposition with the same total incident energy. If the normal incident energy is kept constant, the angular impact with the incident angle up to 45° will produce thin films similar to those produced in normal-angle deposition. However, in general, increasing the angle causes the amount of adhesion (nucleation) of a thin film to decrease. On the other hand, the incident angle does not seem to have a significant effect on the film structure. Another factor, crystallographic orientation, is also found to have little influence on film formation. The amount of damage or deformation of the substrate is also examined. When the cluster beam is deposited on the surface at high enough normal energy, surface damage is seen to increase with increasing angle because of the increasing horizontal momentum of the cluster molecules.

Acknowledgements

The work is supported by the National Science Foundation through grant (CHE-9708049). The authors thank Boris Ni for many helpful discussions.

References

[1] H. Kiitani, N. Toyoda, J. Matsuo, I. Yamada, Nucl. Instr. and Meth. B 121 (1997) 489.
[2] M. Moseler, O. Rattunde, J. Nordiek, H. Haberland, Nucl. Instr. and Meth. B 164–165 (2000) 522.
[3] H. Haberland, M. Karrais, M. Mall, Y. Thurner, J. Vac. Sci. Technol. A 10 (1992) 3266.
[4] H. Haberland, M. Modeler, Y. Qiang, O. Rattunde, T. Reiners, Y. Thurner, Surf. Rev. Lett. 3 (1996) 887.
[5] Y. Qiang, Y. Thurner, T. Reiners, O. Rattunde, H. Haberland, Surf. Coat. Technol. 100/101 (1998) 27.
[6] W. Mahoney, D.M. Schaefer, A. Patil, R.P. Andres, R. Reifenberger, Surf. Sci. 316 (1994) 383.
[7] A. Delcorte, X.V. Eynde, P. Bertrand, D.F. Reich, Nucl. Instr. and Meth. B 157 (1999) 138.
[8] Y. Kataoka, K. Wittmaack, Surf. Sci. 424 (1999) 299.
[9] T. Ohashi, K. Miyake, K. Ohashi, Nucl. Instr. and Meth. B 121 (1997) 40.
[10] S.W. Levine, J.R. Engstrom, P. Clancy, Surf. Sci. 401 (1998) 112.
[11] L. Qi, S.B. Sinnott, J. Phys. Chem. B 101 (1997) 6883.
[12] L. Qi, Susan B. Sinnott, J.Vac. Sci. Technol. A 16 (3) (1998) 1293.
[13] L. Qi, Susan B. Sinnott, Surf. Sci. 398 (1998) 195.
[14] L. Qi, S.B. Sinnott, Nucl. Instr. and Meth. B 140 (1998) 39.
[15] T.A. Plaisted, B. Ni, J.D. Zahrt, S.B. Sinnott, Thin Solid Films 381 (2001) 73.
[16] L. Qi, W.L. Young, S.B. Sinnott, Surf. Sci. 426 (1999) 83.

[17] D.W. Brenner, O.A. Shenderova, J.A. Harrison, S.J. Stewart, B. Ni, S.B. Sinnott, J. Phys.: Condensed Matter 14 (2002) 783.
[18] D.W. Brenner, Phys. Status Solidi (b) 217 (2000) 23.
[19] A.V. Petukhov, A. Fasolino, Phys. Status Solidi (a) 181 (2000) 109.
[20] J. Que, M.W. Randy, P.V. Smith, Phys. Rev. B 60 (12) (1999) 8686.
[21] H.U. Jager, K. Albe, J. Appl. Phys. 88 (2) (2000) 1129.
[22] P. De Sainte Claire, K. Son, W.L. Hase, D.W. Brenner, J.Am. Chem. Soc. 100 (1996) 1761.
[23] Y. Hu, S.B. Sinnott, J. Chem. Phys. 116 (2002) 6738.
[24] T.A. Plaisted, S.B. Sinnott, J. Vac. Sci. Technol. A 19 (1) (2001) 262.
[25] M. Ghaly, K. Nordlund, R.S. Averback, Philos. Mag. A 79 (4) (1999) 795.